Impact of anti-GBM antibodies and glomerular neutrophil activation on glomerulonephritis in experimental MPO-ANCA vasculitis

Go Kanzaki[1,3], Shinya Nagasaka[1], Seiichiro Higo[1], Yusuke Kajimoto[1], Takafumi Kanemitsu[1], Michiko Aoki[1], Kiyotaka Nagahama[1], Yasuhiro Natori[2], Nobuo Tsuboi[3], Takashi Yokoo[3], Akira Shimizu[1]

[1]Department of Analytic Human Pathology, Nippon Medical School, Tokyo, Japan

[2]Department of Health Chemistry, School of Pharmacy, Iwate Medical University, Iwate, Japan

[3]Division of Nephrology and Hypertension, Department of Internal Medicine, The Jikei University School of Medicine, Tokyo, Japan

Running title: Glomerular neutrophil activation in AAGN

Word count: 7365 words, Abstract 292 words

Corresponding Author:

Akira Shimizu M.D., Ph.D.

Department of Analytic Human Pathology, Nippon Medical School

1-1-5 Sendagi, Bunkyo-ku, Tokyo 113-8602, Japan

Phone: +81-3-3822-2131; FAX: +81-3-5685-3067; e-mail: ashimizu@nms.ac.jp

ABSTRACT

Background

Antineutrophil cytoplasmic antibody (ANCA) and neutrophil interactions play important roles in ANCA-associated glomerulonephritis (AAGN) pathogenesis. However, mechanisms underlying the pathogenesis of crescent formation in ANCA-associated vasculitis (AAV) have not been completely elucidated. To ascertain the involvement of these interactions in necrotizing crescentic glomerulonephritis (NCGN), we used an AAGN rat model and investigated the effects of the anti-myeloperoxidase (MPO) antibody (Ab) titer, tumor necrosis factor α (TNF-α), granulocyte colony-stimulating factor (G-CSF), and subnephritogenic anti-GBM Abs, as pro-inflammatory stimuli.

Methods

NCGN was induced in Wistar Kyoto rats by human MPO (hMPO) immunization. Renal function, pathology, and glomerular cytokine and chemokine expression were evaluated in hMPO-immunized rats with/without several co-treatments (TNF-α, G-CSF, or subnephritogenic anti-GBM Abs). Rat neutrophils activation by IgG purified from rat serum in each group was examined in vitro.

Results

The hMPO-immunized rats had significantly higher level of anti-hMPO Ab production. The induced anti-hMPO Abs cross-reacted with TNF-α- or G-CSF-primed rat neutrophils secreting TNF-α and interleukin-1β in vitro. The reactivity of anti-MPO Abs against rat MPO, crescent formation with

neutrophil extracellular traps, and glomerular-activated neutrophil infiltration in the rat model were significantly enhanced by subnephritogenic anti-GBM Ab but not by TNF-α or G-CSF administration. The model rats injected with the subnephritogenic anti-GBM Abs showed increased urinary albumin excretion and serum TNF-α, CXCL1, and CXCL2 levels. TNF-α, CXCL1, CXCL2, and CXCL8 increased in the glomeruli with significant amounts of crescent formation. In addition, in vitro, activated neutrophils decreased CXCR1 and CXCR2 expressions.

Conclusions

The co-existence of subnephritogenic anti-GBM antibodies leads to the inflammatory environment in glomeruli that is amplified by the interaction of ANCA and neutrophils. Development of NCGN in MPO-AAV may be necessary for not only the accumulation of neutrophils in glomeruli but also the aberrant neutrophil activation on glomerulonephritis.

KEYWORDS

ANCA; neutrophil; chemokine; chemokine receptor; necrotizing crescentic glomerulonephritis;

Short summary

Recent studies have indicated that the interactions between ANCA and neutrophils are pathogenesis of ANCA-associated vasculitis. We examined the involvement of these interactions in necrotizing crescentic glomerulonephritis (NCGN) using a rat model. We found that the presence of subnephritogenic anti-GBM antibodies leads to the inflammatory environment in glomeruli that is amplified by the interaction of ANCA and neutrophils. The aberrantly activated neutrophils on glomerulonephritis were needed to develop NCGN.

Alphabetical list of abbreviations

Antineutrophil cytoplasmic antibody (ANCA); ANCA-associated vasculitis (AAV); ANCA-associated glomerulonephritis (AAGN); anti-glomerular basement membrane antibody (anti-GBM Ab); blood urea nitrogen (BUN); creatinine (Cr); chemokine (C-X-C) ligand (CXCL); CXC chemokine receptor (CXCR); 4′, 6-diamidino-2-phenylindole (DAPI); fluorescein isothiocyanate (FITC); granulocyte colony-stimulating factor (G-CSF); human MPO (hMPO); horseradish peroxidase (HRP); interleukin-1β (IL-1β); myeloperoxidase (MPO); necrotizing crescentic glomerulonephritis (NCGN); neutrophil extracellular traps (NETs); optical density (OD);

tumor necrosis factor α (TNF-α); Wistar Kyoto (WKY)

INTRODUCTION

Antineutrophil cytoplasmic antibodies (ANCA) are autoantibodies found in the serum of necrotizing vasculitis patients with few immune deposits; it predominantly affects small vessels. Its major clinicopathological variants are granulomatosis with polyangiitis, microscopic polyangiitis, and eosinophilic granulomatosis with polyangiitis (1). These autoantibodies are mainly directed against the antigens myeloperoxidase (MPO) or proteinase 3 in the primary granules of neutrophils. Although two types of ANCA are associated with the three variants of ANCA-associated vasculitis (AAV), the clinical manifestations caused by necrotizing vasculitis, such as diffuse alveolar hemorrhage or necrotizing crescentic glomerulonephritis (NCGN), are shared among all variants of AAV. Importantly, MPO-ANCA-positive patients with renal involvement have the worst survival rates (2). However, underlying mechanisms of NCGN development pathogenesis in MPO-AAV have not been completely elucidated.

Several recent studies have implied that MPO-ANCA directly causes NCGN by cytokine-primed neutrophil activation (3–6). Several animal models have indicated that MPO-ANCA is indeed pathogenic. Xiao et al. demonstrated that anti-MPO Abs raised by immunizing MPO-deficient mice with murine MPO caused NCGN after injection into wild-type mice (4). Little et al. also demonstrated that Wistar Kyoto (WKY) rats immunized with human MPO (hMPO) developed Abs that cross-reacted with rat MPO and caused pauci-immune NCGN, 8 weeks after immunization (5). These models were based on the production of Abs to MPO transferred or

generated in rodents. However, the disease activity of these rodent models was relatively mild (7). Similarly, in clinical research studies, controversial data exist regarding ANCA pathogenicity; the ANCA titers do not positively correlate with disease activity, and naturally occurring ANCA can be detected in healthy individuals (8, 9). Interestingly, although AAV is widely accepted as a systematic disease, ANCA-positive renal-limited vasculitis has also been reported (10). Therefore, we believe that additional factors are involved in NCGN development in AAV.

Several studies have suggested that neutrophils play an important role in ANCA-associated glomerulonephritis (AAGN) pathogenesis (11, 12). It is well known that MPO-ANCA can activate neutrophils primed by proinflammatory cytokines, such as tumor necrosis factor-α (TNF-α) (13, 14) or granulocyte colony-stimulating factor (G-CSF) (15, 16), to release reactive oxygen species, lytic proteases, and inflammatory cytokines. ANCA also activates neutrophils by inducing a unique type of neutrophil-related cell death characterized by the formation of neutrophil extracellular traps (NETs). Several studies have indicated that NETs occur in patients with AAV and cause tissue damage or capillary inflammation (17).

Conversely, anti-glomerular basement membrane antibodies (anti-GBM Abs) have been used in the MPO-ANCA model to induce accumulation of neutrophils, CD4 positive cells, and macrophages (18). In addition, recent studies have demonstrated that subnephritogenic anti-GBM Abs induced significant numbers of crescentic glomeruli in MPO-ANCA models (19, 20).

Hence, in this study, we used the experimental AAV rat model as previously described (5)

via hMPO immunization and investigated the effects of the anti-MPO Ab titers, TNF-α, G-CSF, and subnephritogenic anti-GBM Abs on NCGN development.

MATERIALS AND METHODS

Animals

We obtained inbred male WKY rats (Charles River Japan, Kanagawa, Japan) weighing approximately 100 g. The rats were housed under specific pathogen-free conditions and were allowed free access to food and water during the experiment. The study protocol was approved by the animal ethics review committee of Nippon Medical School.

AAV Rat model

Experimental AAV was induced in WKY rats as reported previously (5, 14). Briefly, WKY rats were immunized with purified hMPO (Elastin Products Company, Inc., Owensville, MO, USA) in complete Freund's adjuvant (CFA) with the addition of killed Mycobacterium tuberculosis (4 mg/ml) (Chondrex Inc., Redmond, WA, USA) (n = 6 in each group). The hMPO solution was dissolved in phosphate-buffered saline (160, 320, and 640 µg/ml for immunization of rats with 400, 800, and 1600 µg/kg, respectively) and emulsified with an equal volume of CFA (250 µl/rat, respectively). Control rats (n = 6) were immunized with ovalbumin (OVA) in an equal volume of CFA. The hMPO- and OVA-sensitized rats also received 800 ng of pertussis toxin (List Biological Laboratories Inc., Campbell, CA, USA) intraperitoneally on days 0 and 2. All rats were sacrificed 8 weeks after hMPO immunization; blood, urine samples, and tissues were obtained.

Animal groups

To investigate the effects of the ANCA titers, TNF-α, G-CSF, and subnephritogenic anti-GBM Ab on glomerular lesions, the present study comprised two experiments (Table 1).

The first experiment examined the effects of the hMPO dose. WKY rats were immunized with various hMPO doses: (i) 400 μg/kg, (ii) 800 μg/kg, (iii) 800 μg/kg prime/boost on day 28 (800 μg/kg ×2), and (iv) 1,600 μg/kg.

In the second experiment for co-treatment studies, rats immunized with 1,600 μg/kg of hMPO on day 0 were divided into three additional experimental groups: (iv) the hMPO-alone group, in which hMPO-immunized rats did not receive any type of treatment; (v) the G-CSF group, in which hMPO-immunized rats received 20 μg human G-CSF (Kyowa Hakko Kirin, Co., Ltd., Tokyo, Japan) subcutaneously on days 28–56 (21); (vi) the TNF-α group, where hMPO-immunized rats received 1.0 μg TNF-α (Biolegend, San Diego, CA, USA) intravenously on days 28, 35, 42, and 49 (22); and (vii) the anti-GBM Ab (hMPO) group, where hMPO-immunized rats were intravenously injected with 0.25 μg subnephritogenic anti-GBM Abs on day 28. Another group was added as a control for the anti-GBM Ab (hMPO) group: (viii) the anti-GBM Ab (OVA) group, in which OVA-immunized rats were intravenously injected with 0.25 μg subnephritogenic anti-GBM Abs on day 28.

Histological and immunohistochemical analyses

For light microscopy examinations, renal tissues were fixed in 10% neutral-buffered formalin and embedded in paraffin. Sections were subjected to hematoxylin and eosin staining and periodic acid-Schiff staining for histopathological examination. Naphthol AS-D chloroacetate esterase staining was performed to detect infiltrating neutrophils. According to the ISN/RPS 2003 classification of lupus nephritis, crescentic glomerular lesions are defined by the presence of at least two cell layers of proliferation in Bowman's space (23). The number of glomerular crescents is expressed as the mean percentage of glomeruli with crescents in 50 glomeruli in each rat. Neutrophil accumulation was quantified by the mean number of naphthol AS-D chloroacetate esterase-positive cells per glomerulus in 50 glomerular cross-sections. Microvascular lung hemorrhage was visualized by Perls' Prussian blue staining for ferric iron.

In immunofluorescence studies, the glomerular deposition of IgG and C3 were examined by fluorescein isothiocyanate (FITC)-labeled goat anti-rat IgG Abs (MBL, Nagoya, Japan) and anti-rat C3 Abs (ICN Pharmaceuticals, Bryan, OH, USA), respectively. NETs in the glomerular crescents were assessed by direct immunofluorescence using a FITC-conjugated mouse anti-rat MPO Ab (Novus Biologicals, Littleton, CO, USA) and 4′, 6-diamidino-2-phenylindole (DAPI) (VECTASHIELD H-1200; Vector Laboratories, Burlingame, CA, USA) as previously described (24, 25). The images of the NETs were acquired using a TCS SPE confocal laser scanning microscope with the LAS AF lite software program (Leica, Wetzlar, Germany).

For electron microscopy examination, the kidney tissue was fixed in a 2.5% glutaraldehyde

solution in phosphate buffer (pH 7.4) and post-fixed with 1% osmium tetroxide and embedded in Epok 812. Ultrathin sections were stained with uranyl acetate and lead citrate and examined with an electron microscope (model H7100; Hitachi Corp., Tokyo, Japan).

Activation of bone marrow-derived cells by IgG purified from the AAV rat model

For isolating bone marrow cells, the femurs and tibias were removed from 4–8-week-old WKY rats. The bone marrow was flushed out into a new petri dish with 10 ml of RPMI supplemented with 10% fetal bovine serum. Contaminating erythrocytes were lysed, and the cells were washed and resuspended in the culture medium at 1.0 × 107 cells/dish. After 5% CO2 incubation at 37°C for 1 h, floating cells were collected, density was regulated, and culture was added to a 96-well plate at 2.5 × 106 cells/well, which was replenished with 200 µL fresh culture medium. Neutrophils and monocytes comprised >90% cells obtained by this method.

The bone marrow-derived cells were primed with TNF-α (2 ng/ml) or G-CSF (500 µg/ml), incubated at 37°C for 30 min, and treated with 100 µg/ml of IgG purified from rat serum using a protein G column (Protenova Co., Ltd., Tokushima, Japan). After incubation for 4 h at 37°C, the culture supernatants for ELISA and cells for quantitative real-time PCR were collected. Analysis of unstimulated cells provided baseline values (3, 26–28).

Quantification of anti-MPO Abs

The hMPO Ab responses were evaluated by conventional ELISA. Briefly, hMPO (0.5 μg/ml) was coated on 96-well plates and left overnight at 4°C; the wells were then blocked with 25% Block Ace (DS PharmaBiomedical Co., Ltd., Osaka, Japan). After washing, the serum samples (1:1,000) were incubated with hMPO at 4°C overnight, and then incubated with horseradish peroxidase (HRP)-conjugated goat anti-rat IgG Abs (1:1,000) for 60 min at room temperature as the secondary Ab. A tetramethylbenzidine substrate was added and optical density (OD) was quantified at 450 nm. Anti-hMPO Ab was detected in serial dilution of the rat serum at 8 weeks after immunization.

To demonstrate that the induced anti-hMPO Abs cross-reacted with rat neutrophils, the anti-rat MPO Abs were similarly measured by ELISA. Briefly, rat MPO (Hycult Biotechnology, Uden, Netherlands) was coated at 0.5 μg/ml. The serum samples (1:100) were incubated at 4°C overnight. HRP-conjugated goat anti-rat IgG Abs (1:1,000) were used for 60 min at room temperature as the secondary Abs. A tetramethylbenzidine substrate was added, and OD was quantified at 450 nm.

Indirect immunofluorescence using rat serum

Abs against hMPO and rat MPO were detected by indirect immunofluorescence on 4% paraformaldehyde-fixed, Triton-X (0.5%)-permeabilized rat leukocytes. These cells were blocked with 5% bovine serum albumin, and then blocked with the culture supernatant from

hybridoma-producing anti-Fc-receptor Abs (clone 2.4G2, ATCC). The serum from the rats immunized with hMPO alone was diluted 1:100, and Alexa Fluor 594 donkey anti-rat IgG (Life Technologies, Inc., Carlsbad, CA, USA) was used as the secondary Ab. The samples were also examined under a confocal laser scanning microscope.

Isolation of rat glomeruli

Rats were decapitated under ether anesthesia and kidneys were collected. The glomeruli were isolated by a differential sieving method as described previously (29, 30). Under light microscopy, tubular contamination was <5%.

Real-time quantitative PCR

The mRNA expression of TNF-α, interleukin (IL)-1β, chemokine (C-X-C) ligand 1 (CXCL1), CXCL2, CXCL8, CXC chemokine receptor 1 (CXCR1), and CXCR2 was detected using THUNDERBIRD SYBR qPCR Mix (TOYOBO, Osaka, Japan) based on real-time detection of accumulated fluorescence, according to manufacturer's instructions (ABI PRISM 7900HT; Applied Biosystems, Carlsbad, CA, USA). The total RNA of isolated glomeruli or activating neutrophils were extracted using ISOGEN (Nippon Gene, Tokyo, Japan), according to manufacturer's protocol. cDNA was synthesized using a High Capacity cDNA Reverse Transcription kit (Applied Biosystems), according to manufacturer's instructions. The sequences of the real-time PCR primers used in this

study are shown in Supplementary Table 1. Samples were normalized by the housekeeping gene, β-actin, or 18S.

Cytokines in serum or culture supernatant

The concentrations of rat TNF-α, CXCL1, and CXCL2 in rat serum and TNF-α and IL-1β in activated neutrophil culture supernatant were measured by ELISA, according to manufacturer's protocol (TNF-α, IL-1β: eBioscience, San Diego, CA, USA; CXCL1, CXCL2: R&D Systems Inc., Minneapolis, MN, USA).

Urine and blood analyses

The rats were placed in metabolic cages one day before sacrifice, and urine was collected for 24 h. The urine was tested by dipstick-method for hematuria and proteinuria, and the extent was expressed as the mean on a scale of 0 (none) to 4 (severe) for hematuria and 0 (none) to 5 (severe) for proteinuria. Albuminuria was determined by a rat albumin ELISA quantitation kit (Bethyl Laboratories Inc., Montgomery, TX, USA). Peripheral blood and serum samples were collected at sacrifice time. Total white blood cells (WBC) were counted using an automatic blood cell counter (PCE-210; Erma, Tokyo, Japan). The serum creatinine (Cr) and blood urea nitrogen (BUN) levels were measured using an autoanalyzer (SRL, Tokyo, Japan). The concentrations of rat MPO in the serum were measured by a specific ELISA method, according to manufacturer's instructions (Hycult

Biotechnology).

Statistical analysis

The data were expressed as mean ± SD and compared with the control group or the hMPO group using one-way analysis of variance and Dunnett's post hoc test. P-value < 0.05 was considered statistically significant. All statistical analyses were performed with SPSS Version 21.0 statistical software package (IBM Corp., Armonk, NY, USA).

RESULTS

Rats immunized with hMPO

In the first experiment, all rats immunized with hMPO developed hematuria after 8 weeks. Degree of hematuria was dose-dependent. None of the controls developed hematuria (Figure 1a). However, degree of proteinuria was not significantly different between the groups (Figure 1b).

Immunization with hMPO led to the development of anti-hMPO Abs. The anti-hMPO Ab productions were significantly higher in the two rat groups immunized with 800 μg/kg prime/boost and 1,600 μg/kg of hMPO. Rats immunized with OVA were negative for anti-hMPO Abs (Figure 1c).

All AAV rat models developed focal and segmental NCGN (Figure 1e). Immunofluorescence microscopy revealed trace/negative staining for IgG and C3 in these kidneys, thus indicating pauci-immune type NCGN (Figure 1f). Although there was a trend toward an increase in crescentic formation with increasing doses of hMPO, the severity of NCGN was mild (approximately 2%–4% of glomeruli had crescents) (Figure 1d). No crescents were seen in control rats immunized with OVA. Lung hemorrhage was observed in several rats immunized with hMPO (Supplementary Figure 1).

The induced anti-hMPO Abs cross-reacted with rat neutrophils

We examined whether anti-hMPO Abs cross-reacted with rat neutrophils. Using indirect immunofluorescence on the rat and human neutrophils, hMPO-ANCA in the serum from

hMPO-immunized rats was found to react not only with human neutrophils but also rat neutrophils (Figure 2a). However, the serum from OVA-immunized rats did not react with either human or rat neutrophils. In addition, hMPO-ANCA in rat serum reacted to rat MPO (OD ratio >2 vs. control serum) as shown by anti-rat MPO ELISA (Figure 2b). Importantly, in comparison with the TNF-α and G-CSF groups, the serum from the anti-GBM Ab (hMPO) group exhibited a higher ELISA OD value for rat MPO.

Co-treatment study to induce significant numbers of crescentic glomeruli

In the second co-treatment study, all rats developed hematuria after 8 weeks (Figure 3a). Urinary albumin excretion was significantly higher in the anti-GBM Ab (hMPO) group than in the hMPO-alone group (123.1 ± 54.5 mg/day vs 5.89 ± 3.61 mg/day in the anti-GBM Ab (hMPO) and hMPO-alone groups, respectively, $P < 0.05$; Figure 3b), although it was not statistically significantly different between the TNF-α or G-CSF groups and the hMPO-alone group.

Next, we examined the serum cytokine levels in these groups. The serum levels of TNF-α were increased in the anti-GBM Ab (hMPO) group (3.0 ± 2.3 ng/ml) and anti-GBM Ab (OVA) group (0.58 ± 0.18 ng/ml), but not in the other experimental groups (Figure 3d). Serum Cr and BUN levels were not significantly different between the groups and remained within normal ranges in all groups (Figure 3c).

As shown in Figure 4, the administration of G-CSF or TNF-α to hMPO-immunized rats

induced focal and segmental crescent formation (2.7% ± 1.2% in the G-CSF group and 3.4% ± 1.2% in the TNF-α group), but did not increase the number of glomeruli with crescent formation. However, subnephritogenic anti-GBM Abs administration led to a high percentage of crescent formation (55.0% ± 14.2% vs 3.0 ± 1.7% in anti-GBM Ab (hMPO) and hMPO-alone groups, respectively, $P < 0.05$; Figures 4a, c). The anti-GBM (OVA) group showed mild crescentic glomerulonephritis (5.0% ± 3.7%). The NETs in the glomerular crescents were assessed by confocal laser scanning microscopy after co-staining with DAPI and MPO. Conversely, the NETs in the glomerular crescents showed a meshwork composed of DNA fibers and MPO in the anti-GBM Ab (hMPO) group (Figure 4b).

The expression of inflammatory cytokine and chemokine receptors in neutrophils

As shown in Figure 5, bone marrow-derived cells primed with TNF-α or G-CSF and stimulated by IgG purified from the model rats showed increased secretion of IL-1β or TNF-α. Notably, IL-1β production maximally increased in the bone marrow cells stimulated by IgG from the anti-GBM Ab (hMPO) group (Figure 5a). Similarly, the cells primed with G-CSF showed increased secretion of TNF-α when stimulated by IgG from rats immunized with hMPO (Figure 5b). Furthermore, according to a real-time PCR analysis of these cells, the expression of IL-1β was increased when stimulated by IgG from the hMPO-alone and anti-GBM Ab (hMPO) groups (Figure 5c). However, TNF-α expression was not significantly increased (Figure 5d).

Next, we examined changes in the chemokine receptors CXCR1 and CXCR2 in neutrophils

following TNF-α priming and anti-hMPO IgG stimulation. In vitro anti-hMPO IgG from model rat serum significantly upregulated the expression of CXCR1 on TNF-α-primed neutrophils (Figure 5e). Contrastingly, the IgG from the anti-GBM Ab (hMPO) group downregulated the expression of CXCR1 and CXCR2 (Figures 5e, f).

The increased number of glomerular neutrophils was insufficient to achieve crescentic formation

WBC counts in peripheral blood and serum levels of rat MPO were markedly elevated in the G-CSF group, although they were not increased in the other groups (WBC: 18.7 × 103 ± 1.7 × 103 vs 7.0 × 103 ± 0.5 × 103 cells/μl, MPO: 82.7 ± 30.3 vs 7.6 ± 4.3 ng /ml, in the G-CSF and anti-GBM Ab (hMPO) groups, respectively, $P < 0.05$; Figures 6a, b). The numbers of esterase-positive neutrophils in the glomeruli were significantly increased in the G-CSF and anti-GBM Ab (hMPO) groups (G-CSF group: 4.2 ± 0.3, anti-GBM Ab (hMPO) group: 2.0 ± 0.5, $P < 0.05$ vs. control). The hMPO-alone and TNF-α groups showed no significant increases in the amount of neutrophils within the glomerulus compared to the OVA control group (Figure 6c). These histological findings with crescent formation are summarized in Table 2. Electron microscopy showed that activated neutrophils in the glomerular capillaries underwent morphological changes. In the hMPO-alone, G-CSF, and TNF-α groups, morphological features of the infiltrated neutrophils were relatively stable, with cells containing various types of granules and lobulated nuclei. Conversely, in the

anti-GBM Ab (hMPO) group, the neutrophils firmly adhered to the swelling endothelial cells, with dramatic morphological changes; the nucleus lost its lobules, the chromatin decondensed, and the granules disintegrated (Figure 6d).

The neutrophil chemoattractant activity in isolated glomeruli may contribute to the aggravation of NCGN.

We analyzed the expression of cytokines and chemokines in isolated glomeruli in each group (Figure 7a–d). Real-time PCR analysis of isolated glomeruli revealed overexpression of cytokines and chemokines, including TNF-α, CXCL1, CXCL2, and CXCL8, was noted in the anti-GBM Ab (hMPO) group. However, these cytokines and chemokines did not significantly increase in the glomeruli in the hMPO-alone, G-CSF, or TNF-α groups. Additionally, we analyzed the rat serum for chemokines using ELISA. The serum CXCL1 and CXCL2 levels both significantly increased in the anti-GBM Ab (hMPO) group (Figures 7e, f).

DISCUSSION

In this study, we demonstrated that all WKY rats immunized with hMPO developed AAGN. Furthermore, in a co-treatment study, the administration of subnephritogenic anti-GBM Abs enhanced the reactivity of anti-MPO Abs against rat MPO and caused a dramatic increase in glomerular crescent formation with urinary albumin excretion. ETs were detected in glomerular crescents in these rats, with numerous infiltrating neutrophils. Additionally, the administered subnephritogenic anti-GBM Abs also enhanced glomerular expressions of TNF-α, CXCL1, CXCL2, and CXCL8 and increased serum levels of TNF-α, CXCL1, and CXCL2, which mainly act as activators and chemoattractants for neutrophils. Notably, TNF-α or G-CSF administration could not induce significant numbers of crescentic glomeruli in the current rat models, despite neutrophil accumulation enhancement in the glomeruli by G-CSF administration. The results of this study indicated that the presence of subnephritogenic anti-GBM antibodies leads to the inflammatory environment in glomeruli that is amplified by the interaction of ANCA and neutrophils. These aberrantly activated neutrophils on glomerulonephritis were needed to develop NCGN.

The inflammatory cells and cytokines are implicated in the pathophysiology of AAV. Several immune cells, such as neutrophils, monocytes/macrophages, and T lymphocytes contribute to the vascular damage (31). These cells infiltrate inflammatory lesions and promote necrotizing vasculitis by several different pathways. Particularly, neutrophils are considered to be one of the primary effector cells in AAGN (11). Many studies have demonstrated that MPO-ANCA can activate

neutrophils primed by proinflammatory cytokines such as TNF-α (13, 14) and G-CSF (16, 32), and cytokine-primed neutrophils may lead to AAGN. ANCA-induced neutrophil activation is greatly enhanced by TNF-α, with a presence of MPO on the outer membrane of neutrophils, thus leading to increased degranulation and an oxidative response. G-CSF not only increases circulating neutrophils numbers but also amplifies several neutrophilic functions, including the ability to adhere to endothelial cells and produce radical oxygen species (33). Based on these findings, we hypothesized that the administration of TNF-α or G-CSF in an AAV rat model can lead to in vivo development of NCGN through neutrophil accumulation and activation in the glomeruli.

We demonstrated that the induced hMPO-ANCA cross-reacted with rat neutrophils in vitro. Additionally, hMPO-ANCA in rat serum could activate the neutrophils primed by TNF-α and G-CSF that produced TNF-α and IL-1β in vitro. The accumulation of neutrophils in the glomeruli was evident after the administration of G-CSF. However, we did not find any significant exacerbation in the crescent formation in TNF-α- or G-CSF-treated rats. Electron microscopy revealed that the morphological features of neutrophils were relatively stable in these groups. We therefore presumed that in vivo stimulation by TNF-α or G-CSF administration in the present study did not lead to any aberrant neutrophil activation. Our findings may indicate that neutrophil accumulation in the glomeruli without sufficient activation may not lead to NCGN development in MPO-AAV.

The subnephritogenic anti-GBM Ab, which alone led to mild NCGN development in this study, could induce significant numbers of crescentic glomeruli, with elevated serum TNF-α, CXCL1,

and CXCL2 levels in AAGN rat model. In the experimental anti-GBM GN, the administration of anti-GBM Abs induced complement activation, chemotactic factor release, and neutrophil-mediated injury (34). In a previous report, 5% of all ANCA-positive serum samples were also positive for anti-GBM Ab, and 32% of all anti-GBM-positive samples had detectable ANCA (35). Srivastava et al. previously reported that double-positive patients have severe renal dysfunction (36). In the present in vitro study, the IgG purified from the hMPO- and subnephritogenic anti-GBM Ab-immunized rats cross-reacted with rat neutrophils that produced more abundant IL-1β than those from the rats immunized by hMPO alone. The significance of IL-1β in AAV has been previously reported (28, 37). These results led us to presume that additional treatment for anti-GBM Abs enhanced anti-rat MPO Abs reactivity.

Recent studies have suggested that the epitope recognition profile or IgG subclass of MPO-ANCA are related to its disease severity (38, 39). We speculate that glomerular inflammation caused by additional anti-GBM Abs led to qualitative changes in rat MPO Ab responses by several possible mechanisms. The first possibility is anti-GBM Abs induce glomerular neutrophil localization, degranulation, and aberrant expression of rat MPO. This could be attributed to the transfer of rat MPO to DCs, which produce polyclonal anti-rat MPO autoantibodies against immunodominant epitopes, and are in turn responsible for pathogenic ANCA production. The second possibility is that the in vivo IgG subclass could be converted to more pathogenic ANCA subclasses by anti-GBM Ab treatment. The third possibility is that anti-GBM Abs may produce other

pathogenic Abs, such as anti-moesin Abs (40), which cross-react with MPO and exacerbate AAGN disease activity. It is presumed that pathogenic ANCA or other Abs induced by anti-GBM Abs also develop crescent formation observed in AAGN.

In renal biopsies from patients with AAV, activated neutrophils are present in affected glomeruli, and the number of activated intraglomerular neutrophils correlates with the severity of renal injury. Additionally, aberrant neutrophil activation is mediated by ANCA that can release NETs (41). These NETs, which are extracellular structures composed of chromatin and granule proteins, trigger AAV and promote autoimmune response against MPO (42). In this study, rats in the anti-GBM (hMPO) group showed increased neutrophils in the glomeruli and NETs formation in glomerular crescents. We therefore concluded that subnephritogenic anti-GBM Abs administration developed NCGN by inducing the aberrant neutrophil activation via endogenous inflammatory cytokines, such as TNF-α and IL-1β, synergistically with MPO-ANCA.

In clinical cases, the histological and clinical features of NCGN in patients with both ANCA and anti-GBM Abs differed from those in patients with either ANCA or anti-GBM Abs alone and showed severe renal involvement and a poor prognosis, similar to that of patients with anti-GBM NCGN (43). In histological findings, Rutgers et al. has showed that periglomerular inflammation was found in only MPO-ANCA– and double-positive patients (44). In our study, neutrophils influx increased in the anti-GBM Ab (hMPO) groups. Regarding the mechanisms underlying the glomerular neutrophil influx, chemokines are important regulators of leukocyte recruitment during

kidney injury (45, 46). CXCL1 and CXCL2 play significant roles in neutrophil recruitment through the CXCR1 and CXCR2 receptors on neutrophils. In a mouse model of MPO-ANCA-mediated NCGN, several chemokines and chemokine receptors, such as CXCL1, CXCL2, and CXCR2, were induced or upregulated (47). A large number of CXCL8- and CXCR1-positive neutrophils are also found in NCGN patients glomeruli (48, 49). Chemokine expression is induced not only by proinflammatory cytokines, such as TNF-α and IL-1β, but also by ANCA (50, 51). To analyze the association between the glomerular neutrophil influx and NCGN, we investigated the expression of chemokines and chemokine receptors in rat neutrophils and isolated glomeruli, respectively. In this study, enhanced CXCL1, CXCL2, and CXCL8 expressions in the glomeruli were noted in the anti-GBM Ab (hMPO) group, which may be associated with NCGN development in MPO-AAV. Interestingly, in our results, the expression of CXCR1 and CXCR2 on neutrophils was significantly decreased by stimulated IgG from the immunized hMPO and subnephritogenic anti-GBM Ab rats in vitro compared with IgG from rats immunized with hMPO alone. CXCR2 previously correlated with neutrophil infiltration in a series of inflammatory diseases (52). A recent study, however, demonstrated that the expression of CXCR1 and CXCR2 on neutrophils is significantly decreased in AAV patients, which increases neutrophil adhesion and impairs their migration through the glomerular endothelium monolayer (53). The temporal induction of CXCR2 in MPO-ANCA-mediated NCGN was restricted to the acute inflammation phase, and blocking CXCR2 increased the glomerular accumulation of neutrophils (47). Our results are consistent with those from

studies showing that CXCR1 and CXCR2 downregulation may lead to activated neutrophils retention in the vascular compartment, thus allowing them to interact with circulating ANCA. The inflammatory conditions caused by subnephritogenic anti-GBM Abs may activate neutrophils via downregulation of CXCR, whereas there CXCL upregulation in the glomerulus. In the present study, however, our results of qPCR analysis in the glomeruli isolated from rat kidney could not exclude the possibility of these chemokine alterations reflecting the number of infiltrating leukocytes rather than the signal produced to recruit and activate those leukocytes.

In conclusion, the results of this study indicate that the coexistence of subnephritogenic anti-GBM Abs provides the local inflammatory environment in glomeruli that is amplified by the interaction of MPO-ANCA and neutrophils. The further activated neutrophils by MPO-ANCA or inflammatory conditions may induce NETs or the release of inflammatory cytokines, leading to NCGN development.

ACKNOWLEDGMENT

We express our special thanks to Mr. Takashi Arai, Ms. Mitue Kataoka, Kyoko Wakamatu, Arimi Ishikawa, and Naomi Kuwahara for their expert technical assistance.

CONFLICT OF INTEREST STATEMENT

The authors declare no conflict of interest.

REFERENCES

(1) Jennette JC, Falk RJ, Bacon PA, et al. 2012 revised International Chapel Hill Consensus Conference Nomenclature of Vasculitides. Arthritis Rheum. 2013;65:1-11.

(2) de Joode AA, Sanders JS, Stegeman CA. Renal survival in proteinase 3 and myeloperoxidase ANCA-associated systemic vasculitis. Clin J Am Soc Nephrol. 2013;8:1709-17

(3) Falk RJ, Terrell RS, Charles LA, Jennette JC. Anti-neutrophil cytoplasmic autoantibodies induce neutrophils to degranulate and produce oxygen radicals in vitro. Proc Natl Acad Sci U S A. 1990;87:4115-9

(4) Xiao H, Heeringa P, Hu P, et al. Antineutrophil cytoplasmic autoantibodies specific for myeloperoxidase cause glomerulonephritis and vasculitis in mice. J Clin Invest. 2002;110:955-63

(5) Little MA, Smyth L, Salama AD, et al. Experimental autoimmune vasculitis: an animal model of anti-neutrophil cytoplasmic autoantibody-associated systemic vasculitis. Am J Pathol. 2009;174:1212-20

(6) Jennette JC, Falk RJ. Pathogenesis of antineutrophil cytoplasmic autoantibody-mediated disease. Nat Rev Rheumatol. 2014;10:463-73

(7) Coughlan AM, Freeley SJ, Robson MG. Animal models of anti-neutrophil cytoplasmic antibody-associated vasculitis. Clin Exp Immunol. 2012;169:229-37

(8) Finkielman JD, Merkel PA, Schroeder D, et al. Antiproteinase 3 antineutrophil cytoplasmic antibodies and disease activity in Wegener granulomatosis. Ann Intern Med. 2007;147:611-9

(9) Land J, Rutgers A, Kallenberg CG. Anti-neutrophil cytoplasmic autoantibody pathogenicity revisited: pathogenic versus non-pathogenic anti-neutrophil cytoplasmic autoantibody. Nephrol Dial Transplant. 2014;29:739-45

(10) Fujimoto S, Uezono S, Hisanaga S, et al. Incidence of ANCA-associated primary renal vasculitis in the Miyazaki Prefecture: the first population-based, retrospective, epidemiologic survey in Japan. Clin J Am Soc Nephrol. 2006;1:1016-22

(11) Xiao H, Heeringa P, Liu Z, et al. The role of neutrophils in the induction of glomerulonephritis by anti-myeloperoxidase antibodies. Am J Pathol. 2005;167:39-45

(12) Schreiber A, Kettritz R. The neutrophil in antineutrophil cytoplasmic autoantibody-associated vasculitis. J Leukoc Biol. 2013;94:623-31

(13) Huugen D, Xiao H, van Esch A, et al. Aggravation of anti-myeloperoxidase antibody-induced glomerulonephritis by bacterial lipopolysaccharide: role of tumor necrosis factor-alpha. Am J Pathol. 2005;167:47-58

(14) Little MA, Bhangal G, Smyth CL, et al. Therapeutic effect of anti-TNF-alpha antibodies in an experimental model of anti-neutrophil cytoplasm antibody-associated systemic vasculitis. J Am Soc Nephrol. 2006;17:160-9

(15) Mantovani A, Cassatella MA, Costantini C, Jaillon S. Neutrophils in the activation and regulation of innate and adaptive immunity. Nat Rev Immunol. 2011;11:519-31

(16) Freeley SJ, Coughlan AM, Popat RJ, Dunn-Walters DK, Robson MG. Granulocyte colony stimulating factor exacerbates antineutrophil cytoplasmic antibody vasculitis. Ann Rheum Dis. 2013;72:1053-8

(17) Sangaletti S, Tripodo C, Chiodoni C, et al. Neutrophil extracellular traps mediate transfer of cytoplasmic neutrophil antigens to myeloid dendritic cells toward ANCA induction and associated autoimmunity. Blood. 2012;120:3007-18

(18) Ruth AJ, Kitching AR, Kwan RY, et al. Anti-neutrophil cytoplasmic antibodies and effector CD4+ cells play nonredundant roles in anti-myeloperoxidase crescentic glomerulonephritis. J Am Soc Nephrol. 2006;17:1940-9

(19) Kobayashi K, Shibata T, Sugisaki T. Aggravation of rat nephrotoxic serum nephritis by anti-myeloperoxidase antibodies. Kidney Int. 1995;47:454-63

(20) Heeringa P, Brouwer E, Klok PA, et al. Autoantibodies to myeloperoxidase aggravate mild anti-glomerular-basement-membrane-mediated glomerular injury in the rat. Am J Pathol. 1996;149:1695-706

(21) Tanaka H, Tokiwa T. Influence of renal and hepatic failure on the pharmacokinetics of recombinant human granulocyte colony-stimulating factor (KRN8601) in the rat. Cancer Res. 1990;50:6615-9

(22) Schwarz M, Taubitz A, Eltrich N, Mulay SR, Allam R, Vielhauer V. Analysis of TNF-mediated recruitment and activation of glomerular dendritic cells in mouse kidneys by compartment-specific flow cytometry. Kidney Int. 2013;84:116-29

(23) Weening JJ, D'Agati VD, Schwartz MM, et al. The classification of glomerulonephritis in systemic lupus erythematosus revisited. Kidney Int. 2004;65:521-30

(24) Kessenbrock K, Krumbholz M, Schönermarck U, et al. Netting neutrophils in autoimmune small-vessel vasculitis. Nat Med. 2009;15:623-5

(25) Nakazawa D, Tomaru U, Yamamoto C, Jodo S, Ishizu A. Abundant neutrophil extracellular traps in thrombus of patient with microscopic polyangiitis. Front Immunol. 2012;3:333

(26) Franssen CF, Huitema MG, Muller Kobold AC, et al. In vitro neutrophil activation by antibodies to proteinase 3 and myeloperoxidase from patients with crescentic glomerulonephritis. J Am Soc Nephrol. 1999;10:1506-15

(27) Harper L, Radford D, Plant T, Drayson M, Adu D, Savage CO. IgG from myeloperoxidase-antineutrophil cytoplasmic antibody-positive patients stimulates greater activation of primed neutrophils than IgG from proteinase 3-antineutrophil cytosplasmic antibody-positive patients. Arthritis Rheum. 2001;44:921-30.

(28) Schreiber A, Pham CT, Hu Y, Schneider W, Luft FC, Kettritz R. Neutrophil serine proteases promote IL-1β generation and injury in necrotizing crescentic glomerulonephritis. J Am Soc Nephrol. 2012;23:470-82

(29) Shimizu A, Masuda Y, Mori T, et al. Vascular endothelial growth factor165 resolves glomerular inflammation and accelerates glomerular capillary repair in rat anti-glomerular basement membrane glomerulonephritis. J Am Soc Nephrol. 2004;15:2655-65

(30) Masuda Y, Shimizu A, Kataoka M, et al. Inhibition of capillary repair in proliferative glomerulonephritis results in persistent glomerular inflammation with glomerular sclerosis. Lab Invest. 2010;90:1468-81

(31) Jennette JC, Falk RJ, Hu P, Xiao H. Pathogenesis of antineutrophil cytoplasmic autoantibody-associated small-vessel vasculitis. Annu Rev Pathol. 2013;8:139-60

(32) Iking-Konert C, Ostendorf B, Foede M, et al. Granulocyte colony-stimulating factor induces disease flare in patients with antineutrophil cytoplasmic antibody-associated vasculitis. J Rheumatol. 2004;31:1655-8

(33) Witko-Sarsat V, Rieu P, Descamps-Latscha B, Lesavre P, Halbwachs-Mecarelli L. Neutrophils: molecules, functions and pathophysiological aspects. Lab Invest. 2000;80:617-53

(34) Cochrane CG, Unanue ER, Dixon FJ. A role of polymorphonuclear leukocytes and complement in nephrotoxic nephritis. J Exp Med. 1965; 122:99-116

(35) Levy JB, Hammad T, Coulthart A, Dougan T, Pusey CD. Clinical features and outcome of patients with both ANCA and anti-GBM antibodies. Kidney Int. 2004;66:1535-40

(36) Srivastava A, Rao GK, Segal PE, Shah M, Geetha D. Characteristics and outcome of crescentic glomerulonephritis in patients with both antineutrophil cytoplasmic antibody and anti-glomerular basement membrane antibody. Clin Rheumatol. 2013;32:1317-22

(37) Ferrario F, Vanzati A, Pagni F. Pathology of ANCA-associated vasculitis. Clin Exp Nephrol. 2013;17:652-8

(38) Roth AJ, Ooi JD, Hess JJ, et al. Epitope specificity determines pathogenicity and detectability in ANCA-associated vasculitis. J Clin Invest. 2013;123:1773-83

(39) Pankhurst T, Nash G, Williams J, et al. Immunoglobulin subclass determines ability of immunoglobulin (Ig)G to capture and activate neutrophils presented as normal human IgG or disease-associated anti-neutrophil cytoplasm antibody (ANCA)-IgG. Clin Exp Immunol. 2011;164:218-26.

(40) Nagao T, Suzuki K, Utsunomiya K, et al. Direct activation of glomerular endothelial cells by anti-moesin activity of anti-myeloperoxidase antibody. Nephrol Dial Transplant. 2011;26:2752-60

(41) Nakazawa D, Shida H, Tomaru U, et al. Enhanced formation and disordered regulation of NETs in myeloperoxidase-ANCA-associated microscopic polyangiitis. J Am Soc Nephrol. 2014;25:990-7

(42) Fuchs TA, Abed U, Goosmann C, et al. Novel cell death program leads to neutrophil extracellular traps. J Cell Biol. 2007;176:231-41

(43) Levy JB, Hammad T, Coulthart A, et al. Clinical features and outcome of patients with both ANCA and anti-GBM antibodies. Kidney Int. 2004;66:1535-40

(44) Rutgers A, Slot M, van Paassen P, et al. Coexistence of anti-glomerular basement membrane antibodies and myeloperoxidase-ANCAs in crescentic glomerulonephritis. Am J Kidney Dis. 2005;46:253-62

(45) Chung AC, Lan HY. Chemokines in renal injury. J Am Soc Nephrol. 2011 ;22:802-9

(46) Segerer S, Nelson PJ, Schlöndorff D. Chemokines, chemokine receptors, and renal disease: from basic science to pathophysiologic and therapeutic studies. J Am Soc Nephrol. 2000;11:152-76

(47) van der Veen BS, Petersen AH, Belperio JA, et al. Spatiotemporal expression of chemokines and chemokine receptors in experimental anti-myeloperoxidase antibody-mediated glomerulonephritis. Clin Exp Immunol. 2009;158:143-53

(48) Cockwell P, Brooks CJ, Adu D, Savage CO. Interleukin-8: A pathogenetic role in antineutrophil cytoplasmic autoantibody-associated glomerulonephritis. Kidney Int. 1999;55:852-63

(49) Segerer S, Henger A, Schmid H, et al. Expression of the chemokine receptor CXCR1 in human glomerular diseases. Kidney Int. 2006;69:1765-73

(50) Lazennec G, Richmond A. Chemokines and chemokine receptors: new insights into cancer-related inflammation. Trends Mol Med. 2010;16:133-44.

(51) Calderwood JW, Williams JM, Morgan MD, Nash GB, Savage CO. ANCA induces beta2 integrin and CXC chemokine-dependent neutrophil-endothelial cell interactions that mimic those of highly cytokine-activated endothelium. J Leukoc Biol. 2005;77:33-43

(52) Nagarkar DR, Wang Q, Shim J, et al. CXCR2 is required for neutrophilic airway inflammation and hyperresponsiveness in a mouse model of human rhinovirus infection. J Immunol. 2009;183:6698-707

(53) Hu N, Westra J, Rutgers A, et al. Decreased CXCR1 and CXCR2 expression on neutrophils in anti-neutrophil cytoplasmic autoantibody-associated vasculitides potentially increases neutrophil adhesion and impairs migration. Arthritis Res Ther. 2011;13:R201

Tables and legends to figures

Table 1.

The experimental design

Abbreviations: hMPO, human myeloperoxidase; OVA, ovalbumin; TNF-α, tumor necrosis factor-α; G-CSF, human granulocyte colony-stimulating factor; anti-GBM Ab, anti-glomerular basement membrane antibodies

Table 2.

Summary of histological findings for each group

Supplementary Table 1.

The real-time PCR primers

Figure 1.

The phenotype of the AAGN model rats generated using various concentrations of hMPO

(a) Hematuria (dipstick: 0–4); (b) proteinuria (dipstick: 0–5); (c) anti-hMPO Ab detected by ELISA; (d) frequency of necrotizing and crescentic glomeruli; (e) periodic acid-Schiff staining of the renal pathology in a rat immunized with 1,600 μg/kg of hMPO with ×200 magnification (left panel) and

×600 magnification (right panel); (f) immunofluorescence of a rat model glomerulus stained for rat IgG (left panel) and C3 (right panel) with ×600 magnification. The data are expressed as the means ± SD; n = 6 for each group. ‡P < 0.05, *P < 0.05 vs. the control group (OVA) or the hMPO 400 μg/ml group, respectively. Abbreviations: AAGN, ANCA-associated glomerulonephritis; ANCA, antineutrophil cytoplasmic antibody; hMPO, human myeloperoxidase; OVA, ovalbumin.

Figure 2.

The rat model immunized with hMPO has serum reactivity for rat MPO

(a) The binding of rat model serum to human and rat neutrophils. Indirect immunofluorescence was performed using 4% paraformaldehyde-fixed, Triton-X (0.5%)-permeabilized human and rat neutrophils. Human neutrophils (top panel) incubated with model rat serum; the binding was detected with Alexa Fluor 594-conjugated anti-rat IgG. Rat neutrophils (lower panel) were incubated with model rat serum; the binding was detected with Alexa Fluor 594-conjugated anti-rat IgG. The left panels show DNA of the neutrophils stained with DAPI. (b) The reactivity of anti-hMPO Abs against rat MPO detected by ELISA. The data are shown as mean ± SD; n = 6 for each group. ‡P < 0.05 vs. hMPO-alone group. Abbreviations: DAPI, 4′, 6-diamidino-2-phenylindole; hMPO, human myeloperoxidase; MPO, myeloperoxidase.

Figure 3.

The phenotype of model rats with AAGN exposed to additional stimuli

(a) Hematuria (dipstick: 0–4); (b) albuminuria; (c) Cr and BUN levels; (d) serum TNF-α levels. The data are expressed as the means ± SD; n = 6 for each group. ‡P < 0.05, *P < 0.05 vs. the hMPO-alone group or for specified comparisons. Abbreviations: AAGN, ANCA-associated glomerulonephritis; ANCA, antineutrophil cytoplasmic antibody; BUN, blood urea nitrogen; Cr, creatinine; hMPO, human myeloperoxidase; TNF-α, tumor necrosis factor α.

Figure 4.

The renal histology in the co-treatment experiments

(a) Periodic acid-Schiff staining of the renal pathology in the co-treatment experiments: G-CSF group (upper), TNF-α group (middle), and anti-GBM Ab (hMPO) group (bottom). Magnifications, ×200 (left panel) and ×600 (right panel). (b) The NETs and neutrophils in the glomeruli of the anti-GBM Ab (hMPO) group; NETs were present in the glomerular crescents. The lower left panel shows immunofluorescent merged images of the NETs (arrows), which were detected by anti-rat MPO Ab (green); DNA was labeled with DAPI (blue). The lower right panel shows neutrophils (arrowheads) in the glomeruli. (c) The frequency of crescentic glomerulonephritis. The data are expressed as mean ± SD; n = 6 for each group. ‡P < 0.05 vs hMPO-alone group. Abbreviations: anti-GBM Ab, anti-glomerular basement membrane antibodies; DAPI, 4′, 6-diamidino-2-phenylindole; G-CSF, granulocyte colony-stimulating factor; hMPO, human

myeloperoxidase; MPO, myeloperoxidase; NETs, neutrophil extracellular traps; TNF-α, tumor necrosis factor α.

Figure 5.

In vitro analysis of cytokine-primed neutrophils stimulated with anti-MPO Abs

The secretion of (a) IL-1β and (b) TNF-α from cytokine-primed neutrophils stimulated by IgG purified from each group. The mRNA levels of (c) IL-1β, (d) TNF-α, (e) CXCR1, and (f) CXCR2 in the neutrophils. The data are expressed as mean ± SD. ‡P < 0.05, *P < 0.05 vs. IgG purified from the control groups or for specified comparisons. Abbreviations: CXCR, CXC chemokine receptor; IL-1β, interleukin-1β; MPO, myeloperoxidase; TNF-α, tumor necrosis factor α.

Figure 6.

In vivo analysis of neutrophils in the AAGN rat model

(a) Peripheral WBC count; (b) serum rat MPO level; (c) glomerular neutrophil influx expressed as the number of infiltrating esterase-positive cells per GCS. The data are expressed as mean ± SD; n = 6 for each group. ‡P < 0.05 vs hMPO-alone group. (d) The typical examples for each group depicted with ×600 magnification (left panel). The esterase-positive cells identified by red staining (arrows). The ultrastructural findings of neutrophils in the glomerulus (right panel, ×10,000 magnification).

The ultrastructural findings of neutrophils in the hMPO-alone (top), G-CSF (upper middle), TNF-α (lower middle), and the anti-GBM Ab (hMPO) groups (bottom). Abbreviations: AAGN, ANCA-associated glomerulonephritis; ANCA, antineutrophil cytoplasmic antibody; anti-GBM Ab, anti-glomerular basement membrane antibodies; GCS, glomerular cross section; G-CSF, granulocyte colony-stimulating factor; hMPO, human myeloperoxidase; MPO, myeloperoxidase; WBC, white blood cell; TNF-α, tumor necrosis factor α.

Figure 7.

The gene expression of cytokines and chemokines in isolated glomeruli from the AAV rat model

Quantification of the mRNA expression levels of (a) TNF-α, (b) CXCL8, (c) CXCL1, and (d) CXCL2. The serum levels of (e) CXCL1 and (f) CXCL2. The data are expressed as mean ± SD; n = 6 for each group. ‡P < 0.05 vs hMPO-alone group. Abbreviations: AAV, ANCA-associated vasculitis; ANCA, antineutrophil cytoplasmic antibody; CXCL, chemokine (C-X-C) ligand; hMPO, human myeloperoxidase; TNF-α, tumor necrosis factor α.

Supplementary Figure 1.

The lung histology in AAV rat model

The lung pathology in a rat immunized with 1,600 μg/kg of hMPO. (a) Macroscopic findings, (b) hematoxylin and eosin stain with ×400 magnification, (c) naphthol AS-D chloroacetate esterase stain

with ×400 magnification. The esterase-positive neutrophils are identified by red staining (arrows). (d) Hematoxylin and eosin and Perls' Prussian blue stains with ×400 magnification. Positive iron staining is indicated by blue deposits (arrows), indicating the evidence of previous hemorrhage. Lung hemorrhage was observed in several rats immunized with hMPO but was not significantly enhanced by subnephritogenic anti-GBM Abs. Abbreviations: AAV, ANCA-associated vasculitis; ANCA, antineutrophil cytoplasmic antibody; hMPO, human myeloperoxidase.

Table 1

Animal Group	Immunization Regimen	
	hMPO or OVA (μg/kg)	Additional administration
Control group	OVA 1600	
(i) hMPO 400	hMPO 400	
(ii) hMPO 800	hMPO 800	
(iii) hMPO 800 X2	hMPO 800	hMPO 800 μg/kg on days 28, s.c.
(iV) hMPO alone group	hMPO 1600	
(v) G-CSF group	hMPO 1600	hG-CSF 20 μg on days 28 to 56, s.c.
(vi) TNF-α group	hMPO 1600	rat TNF1.0 μg on days 28, 35, 42, and 49, i.v.
(vii) a*nti-GBM Ab (hMPO) group*	hMPO 1600	anti-GBM Ab 0.25 μg on days 28 i.v.
(viii) a*nti-GBM Ab (OVA) group*	OVA 1600	anti-GBM Ab 0.25 μg on days 28 i.v.

Table 2

Animal Group	Crescent (%)	Neutrophils/glomerulus
Control group	n.d.	0.48 ± 0.23
(iV) hMPO alone group	3.0 ± 1.7	0.62 ± 0.20
(v) G-CSF group	2.7 ± 1.2	4.25 ± 0.28
(vi) TNF-α group	3.3 ± 1.2	0.74 ± 0.19
(vii) a*nti-GBM Ab (hMPO) group*	55 ± 14	2.0 ± 0.53
(viii) a*nti-GBM Ab (OVA) group*	5.0 ± 3.7	0.85± 0.16

Supplementary Table 1

primer	Primer sequence forward	primer sequence reverse
TNF-α	5’-AAATGGGCTCCCTCTCATCAGTTC-3’	5’-TCTGCTTGGTGGTTTGCTACGAC-3’
IL-1β	5’-TACCTATGTCTTGCCCGTGGAG-3’	5’-ATCATCCCACGAGTCACAGAGG-3’
CXCR1	5’-CATCTTCCGCCAGGCATATAAA-3’	5’-GGGACAGACCACGCAATGTT-3’
CXCR2	5’-CAGCAGTGTTCTGTTGCTAGCCT-3’	5’-CCAAGTGTCTCTTCTGGATCAGTGT-3’
CXCL1	5’-GGCAGGGATTCACTTCAAGA-3’	5’-GCCATCGGTGCAATCTATCT-3’
CXCL2	5’-ATCCAGAGCTTGACGGTGAC-3’	5’-AGGTACGATCCAGGCTTCCT-3’
CXCL8	5’-CCCCCATGGTTCAGAAGATTG-3’	5’-TTGTCAGAAGCCAGCGTTCAC-3’
β-actin	5’-ACCACCATGTACCCAGGCATT-3’	5’-CCACACAGAGTACTTGCGCTCA-3’
18S	5’-GACCGGCGCAAGACGAACCAGAGC-3’	5’-AATAACGCCGCCGCATCGCCAGTC-3’

Figure 1

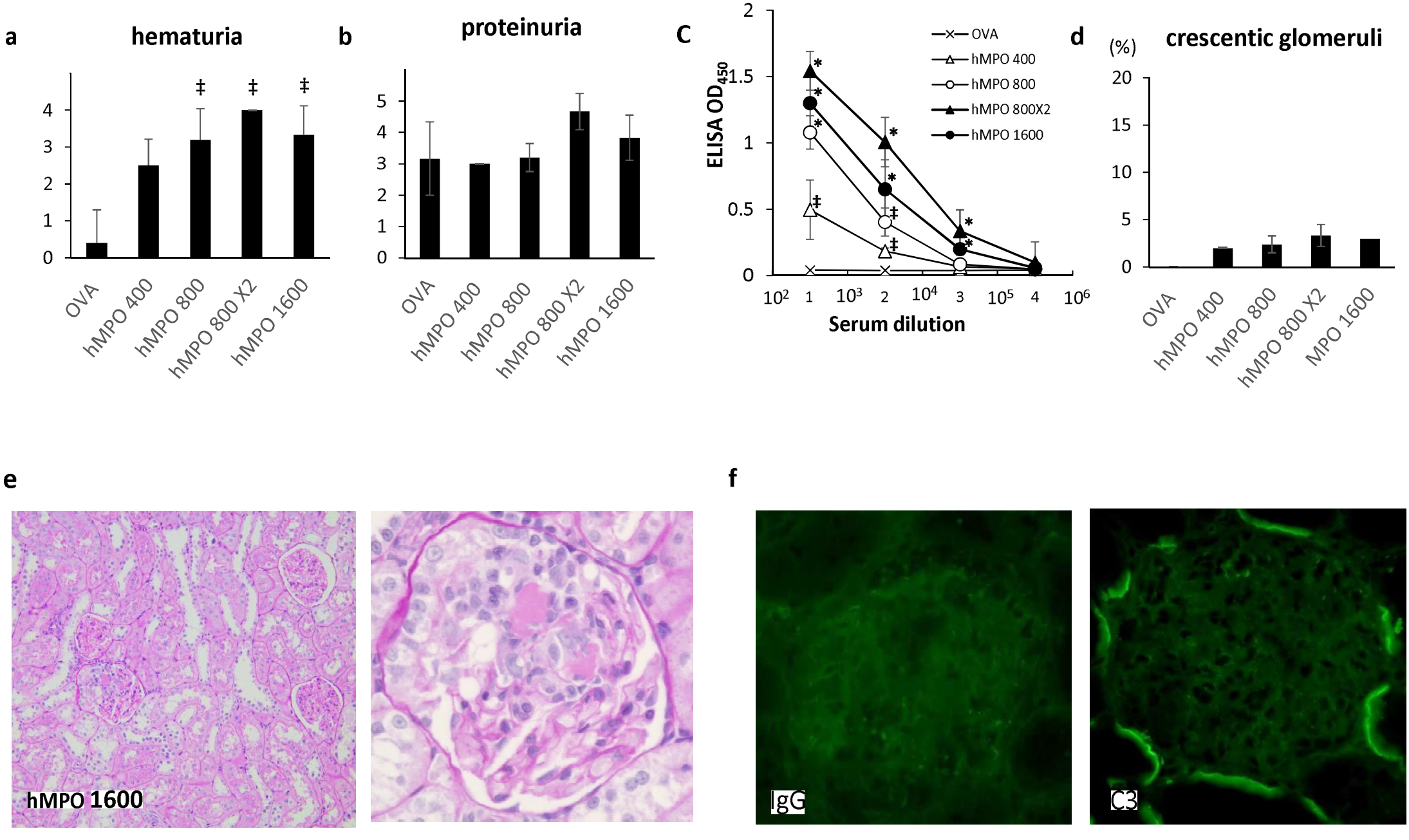
a
hematuria
b
proteinuria
c
ELISA OD450
Serum dilution
OVA
hMPO 400
hMPO 800
hMPO 800X2
hMPO 1600
d
crescentic glomeruli
(%)
OVA
hMPO 400
hMPO 800
hMPO 800 X2
MPO 1600
e
hMPO 1600
f
IgG
C3

Figure 2

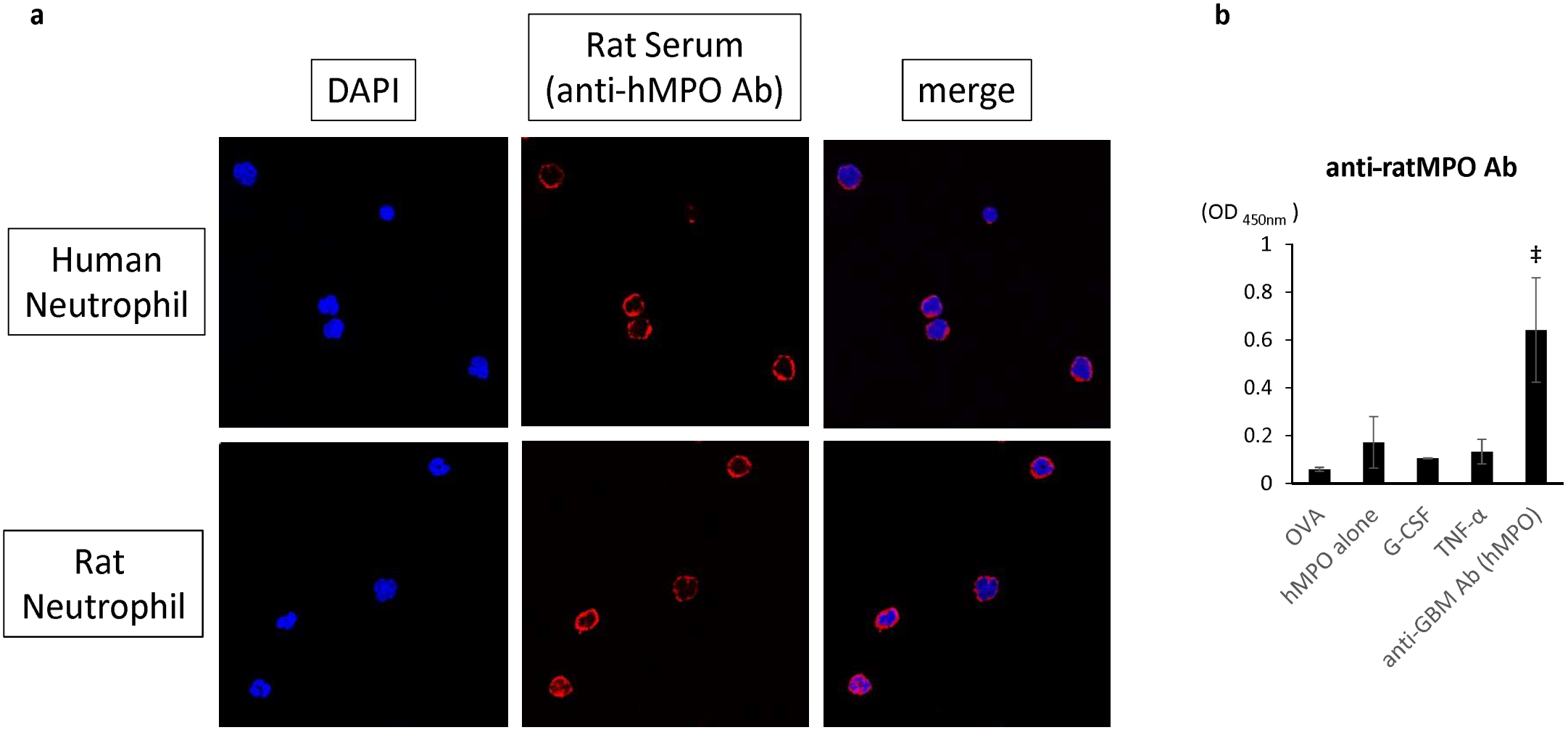
a
DAPI
Rat Serum
(anti-hMPO Ab)
merge
Human
Neutrophil
Rat
Neutrophil
b
anti-ratMPO Ab
(OD 450nm)
1
0.8
0.6
0.4
0.2
0
‡
OVA
hMPO alone
G-CSF
TNF-α
anti-GBM Ab (hMPO)

Figure 3

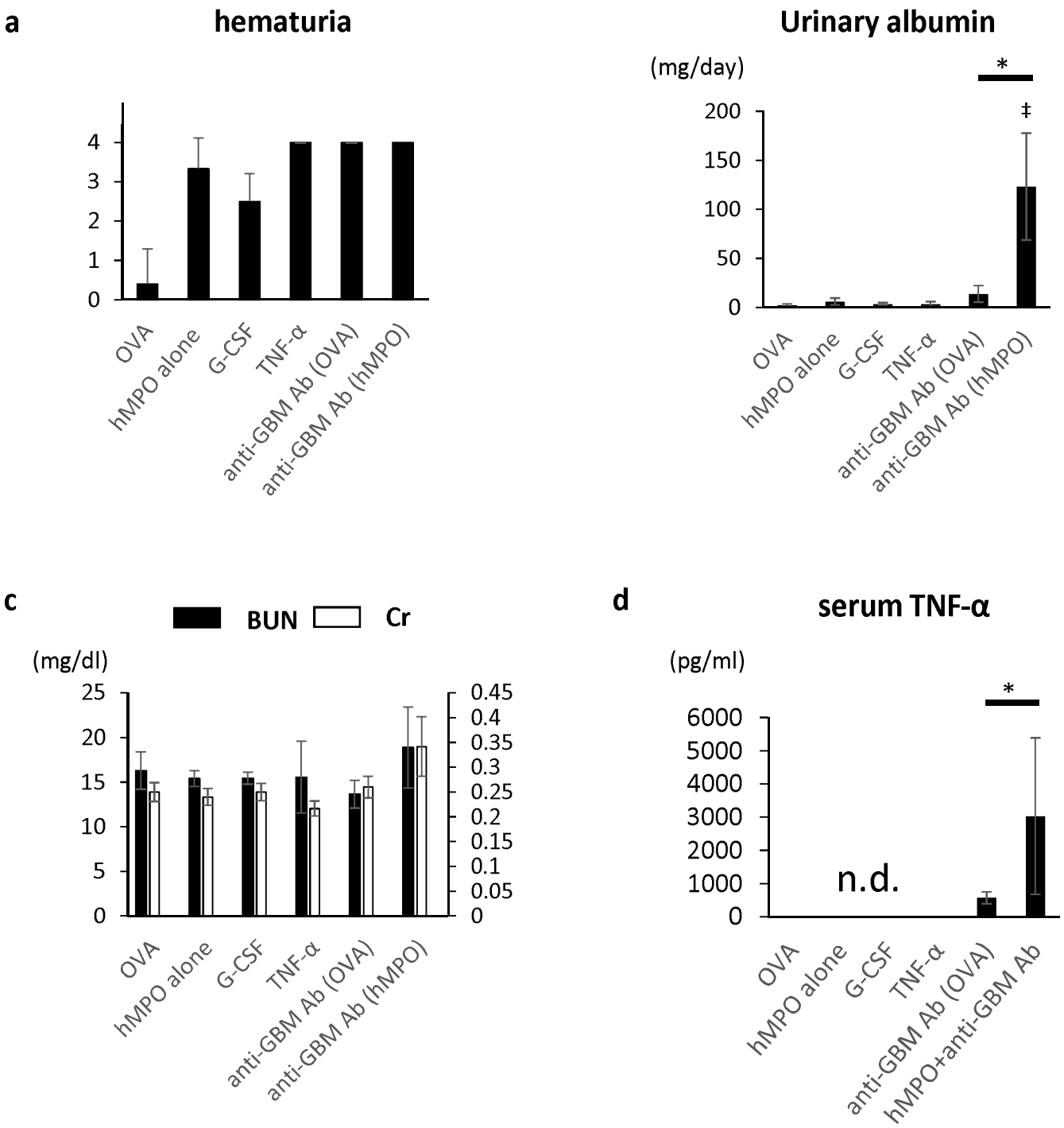
a
hematuria
4
3
2
1
0
OVA
hMPO alone
G-CSF
TNF-α
anti-GBM Ab (OVA)
anti-GBM Ab (hMPO)
Urinary albumin
(mg/day)
*
‡
200
150
100
50
0
OVA
hMPO alone
G-CSF
TNF-α
anti-GBM Ab (OVA)
anti-GBM Ab (hMPO)
c
BUN
Cr
(mg/dl)
25
20
15
10
5
0
0.45
0.4
0.35
0.3
0.25
0.2
0.15
0.1
0.05
0
OVA
hMPO alone
G-CSF
TNF-α
anti-GBM Ab (OVA)
anti-GBM Ab (hMPO)
d
serum TNF-α
(pg/ml)
*
6000
5000
4000
3000
2000
1000
0
n.d.
OVA
hMPO alone
G-CSF
TNF-α
anti-GBM Ab (OVA)
hMPO+anti-GBM Ab

Figure 4

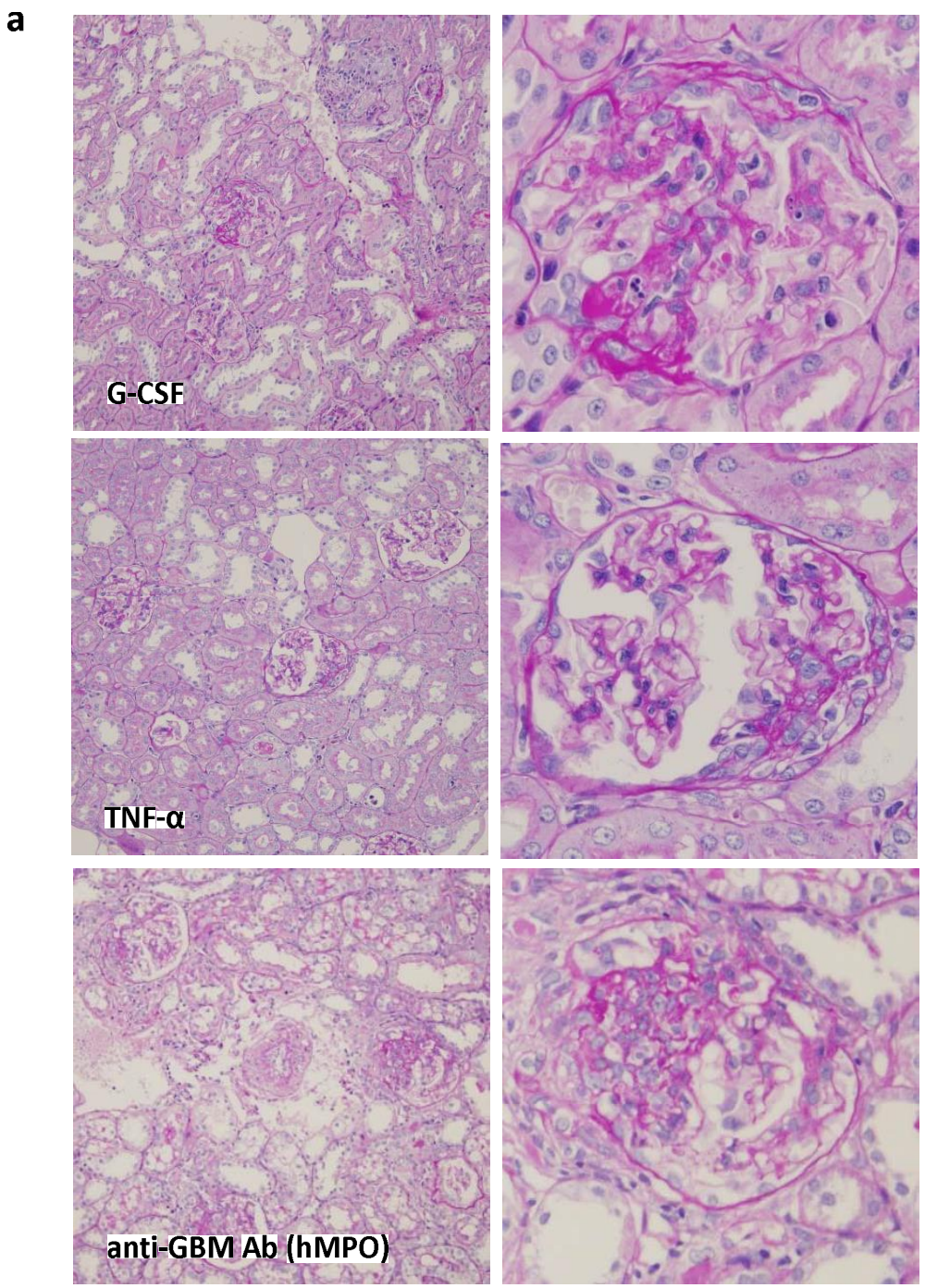
a
G-CSF
TNF-α
anti-GBM Ab (hMPO)
b
MPO
DAPI
merge
neutrophils
c
crescentic glomeruli
(%)
80
60
40
20
0
‡
OVA
hMPO alone
G-CSF
TNF-α
anti-GBM Ab (OVA)
anti-GBM Ab (hMPO)

Figure 5

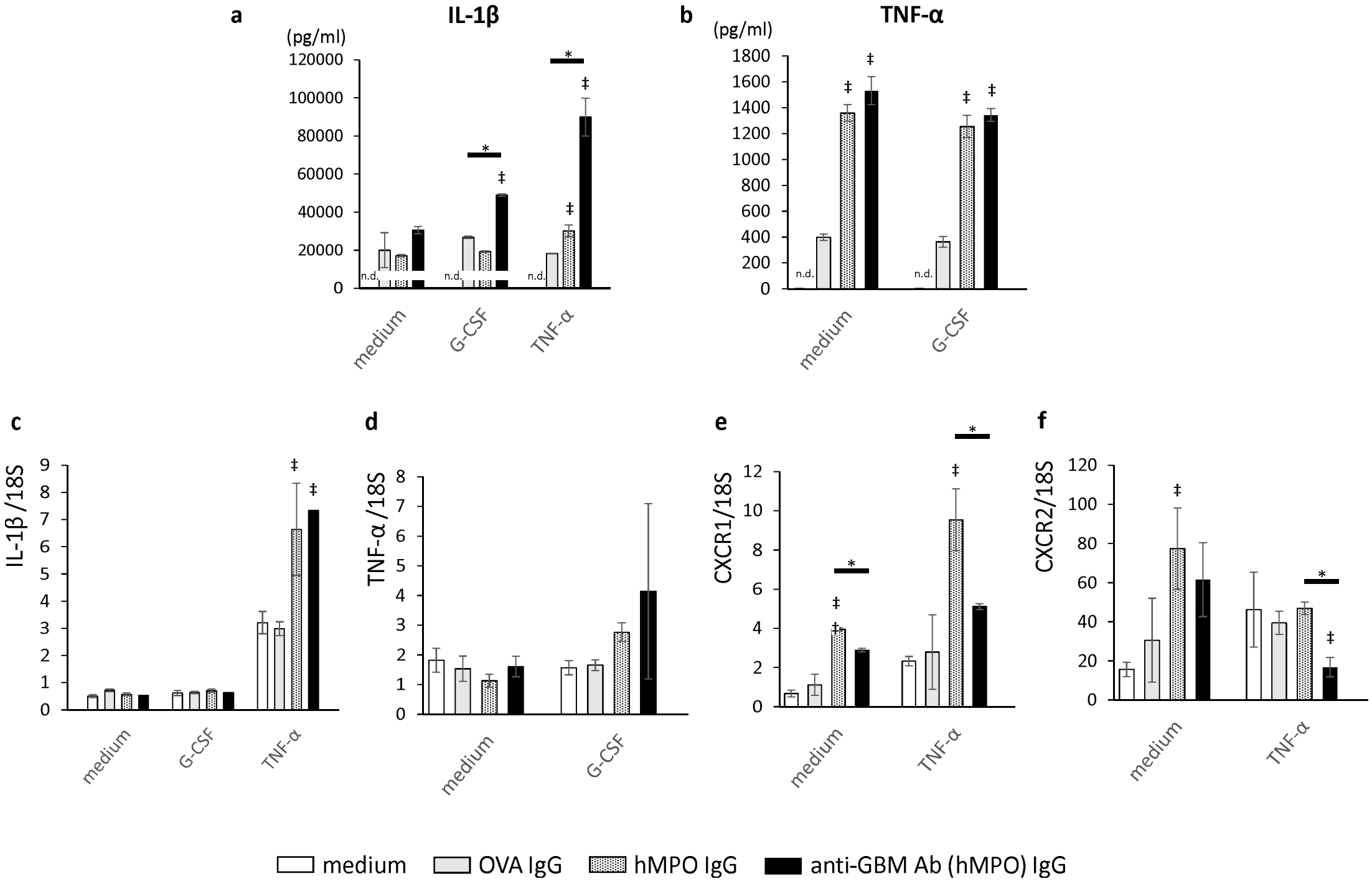
a
IL-1β
(pg/ml)
120000
100000
80000
60000
40000
20000
0
n.d.
*
‡
medium
G-CSF
TNF-α
b
TNF-α
(pg/ml)
1800
1600
1400
1200
1000
800
600
400
200
0
c
IL-1β /18S
d
TNF-α /18S
e
CXCR1/18S
f
CXCR2/18S
medium
OVA IgG
hMPO IgG
anti-GBM Ab (hMPO) IgG

Figure 6

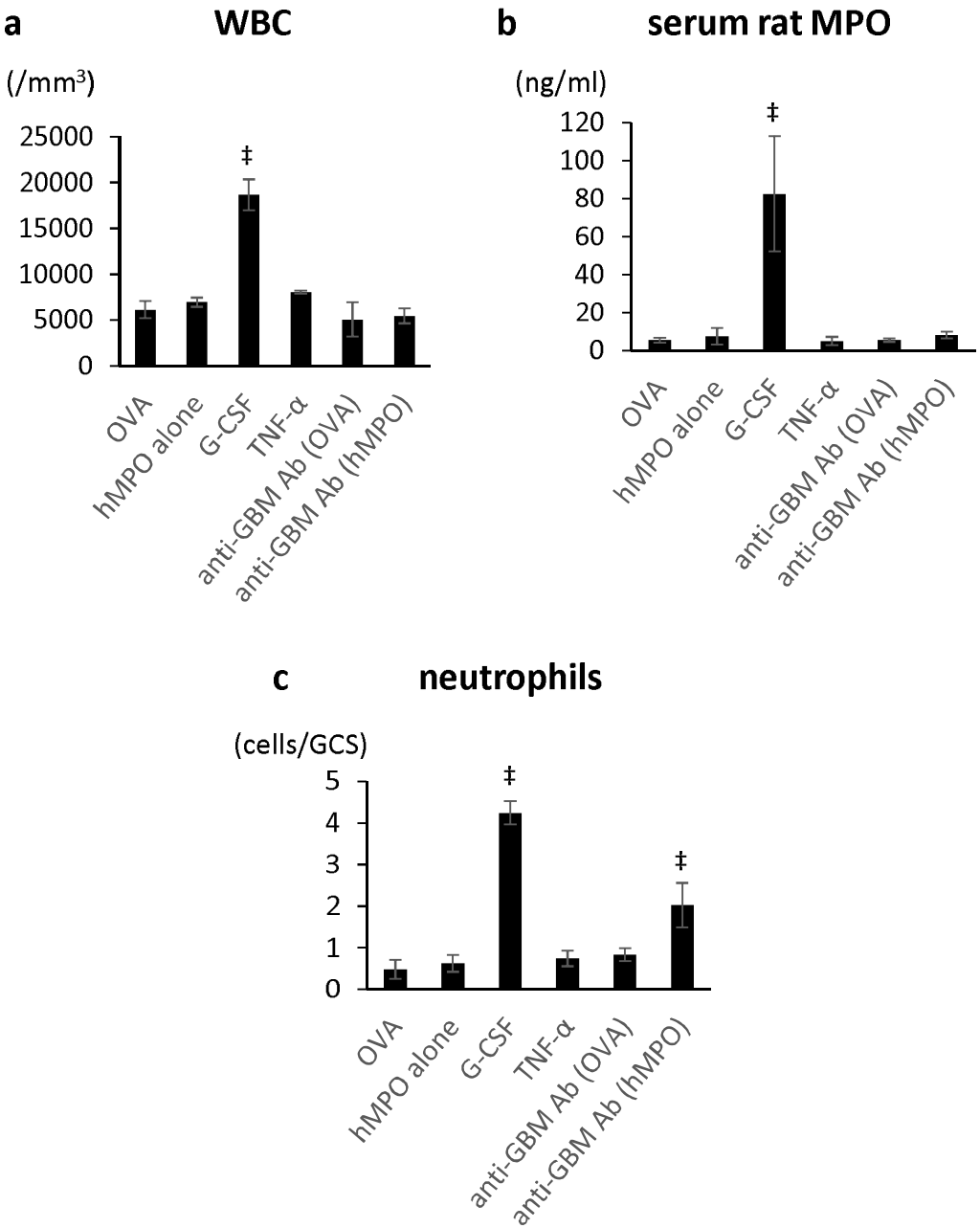
a
WBC
(/mm3)
25000
20000
15000
10000
5000
0
‡
OVA
hMPO alone
G-CSF
TNF-α
anti-GBM Ab (OVA)
anti-GBM Ab (hMPO)
b
serum rat MPO
(ng/ml)
120
100
80
60
40
20
0
‡
OVA
hMPO alone
G-CSF
TNF-α
anti-GBM Ab (OVA)
anti-GBM Ab (hMPO)
c
neutrophils
(cells/GCS)
5
4
3
2
1
0
‡
‡
OVA
hMPO alone
G-CSF
TNF-α
anti-GBM Ab (OVA)
anti-GBM Ab (hMPO)

d

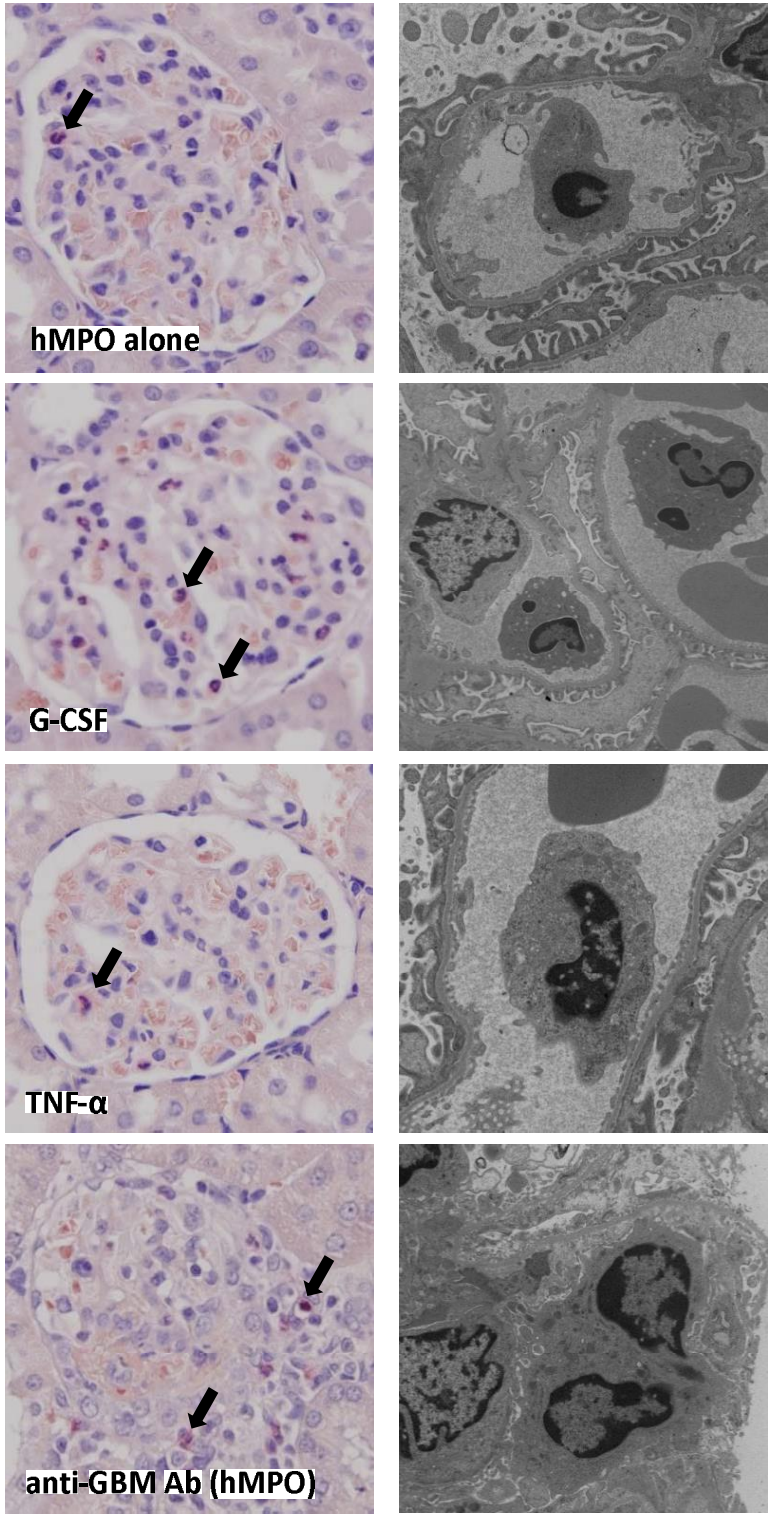
hMPO alone
G-CSF
TNF-α
anti-GBM Ab (hMPO)

Figure 7

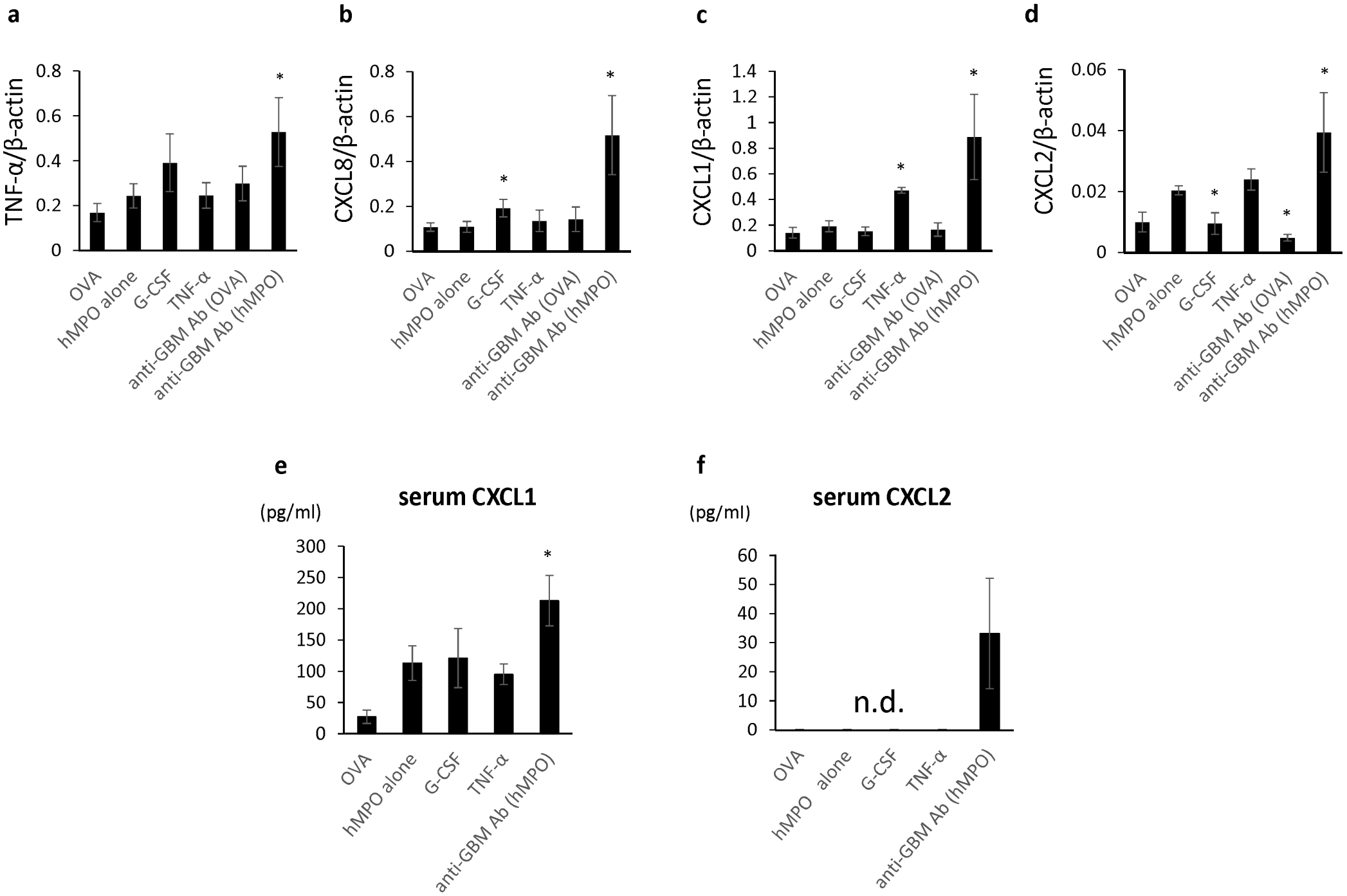
a
TNF-α/β-actin
0.8
0.6
0.4
0.2
0
*
OVA
hMPO alone
G-CSF
TNF-α
anti-GBM Ab (OVA)
anti-GBM Ab (hMPO)
b
CXCL8/β-actin
0.8
0.6
0.4
0.2
0
*
*
OVA
hMPO alone
G-CSF
TNF-α
anti-GBM Ab (OVA)
anti-GBM Ab (hMPO)
c
CXCL1/β-actin
1.4
1.2
1
0.8
0.6
0.4
0.2
0
*
*
OVA
hMPO alone
G-CSF
TNF-α
anti-GBM Ab (OVA)
anti-GBM Ab (hMPO)
d
CXCL2/β-actin
0.06
0.04
0.02
0
*
*
*
OVA
hMPO alone
G-CSF
TNF-α
anti-GBM Ab (OVA)
anti-GBM Ab (hMPO)
e
serum CXCL1
(pg/ml)
300
250
200
150
100
50
0
*
OVA
hMPO alone
G-CSF
TNF-α
anti-GBM Ab (hMPO)
f
serum CXCL2
(pg/ml)
60
50
40
30
20
10
0
n.d.
OVA
hMPO alone
G-CSF
TNF-α
anti-GBM Ab (hMPO)

Supplementary Figure 1